

## PICTORIAL REVIEW

# Pre-operative CT angiography and three-dimensional image post processing for deep inferior epigastric perforator flap breast reconstructive surgery

<sup>1</sup>D L LAM, MD, <sup>1</sup>L M MITSUMORI, MD, <sup>2</sup>P C NELIGAN, MD, <sup>1</sup>B H WARREN, MD, <sup>1</sup>W P SHUMAN, MD and <sup>1</sup>T J DUBINSKY, MD

<sup>1</sup>Department of Radiology, University of Washington Medical Center, Seattle, WA, USA, and <sup>2</sup>Center for Reconstructive Surgery, University of Washington School of Medicine, Department of Surgery, Seattle, WA, USA

**ABSTRACT.** Autologous breast reconstructive surgery with deep inferior epigastric artery (DIEA) perforator flaps has become the mainstay for breast reconstructive surgery. CT angiography and three-dimensional image post processing can depict the number, size, course and location of the DIEA perforating arteries for the pre-operative selection of the best artery to use for the tissue flap. Knowledge of the location and selection of the optimal perforating artery shortens operative times and decreases patient morbidity.

Received 4 June 2012  
Revised 14 August 2012  
Accepted 20 August 2012

DOI: 10.1259/bjr/30590223

© 2012 The British Institute of Radiology

Deep inferior epigastric artery perforator (DIEP) flap surgery for autologous breast reconstruction involves the transfer of the patient's own skin and subcutaneous tissues from the lower abdominal wall to the chest to form the breast mound. The advantage of the DIEP flap technique is that the operation spares the rectus muscle, which results in fewer complications and a faster return to normal activities [1].

The arterial supply to the lower abdominal wall is from the deep inferior epigastric artery (DIEA) and its perforator branches that pass through the rectus muscle to reach the subcutaneous fat and skin. Selecting the portion of the lower abdominal wall to use for the DIEP flap is based on the location, morphology and size of the perforating arteries present. Because the vascular anatomy of the abdominal wall varies greatly both between individuals and between the right and left abdomen within an individual, pre-operative imaging facilitates the surgical dissection by allowing the selection of the area of the lower abdominal wall with the best arterial supply to use for the breast reconstruction [2]. CT angiography (CTA) with three-dimensional (3D) image reconstruction has been successfully implemented for the pre-operative planning of DIEP flap breast reconstructive surgery. Pre-operative availability of 3D reconstructed CT images improves operative outcomes and shortens operation times [3–5]. The objectives of this article are to review the arterial anatomy of the anterior abdominal wall, describe the features used to select a perforator artery for DIEP flap surgery and present a CT scanning and image post-processing protocol.

## Vascular anatomy of the anterior abdominal wall

There are three general branching patterns of the DIEA: Type 1, a single vessel; Type 2, a bifurcated vessel; and Type 3, a trifurcated vessel (Figure 1). Knowing the branching pattern is important to select the vessel branch to include with the vascular pedicle of the DIEP flap. When several suitable perforators are present, depiction of the DIEA defines whether the suitable perforators emanate from and can be harvested with the same source vessel. Perforator origin is also important for predicting flap perfusion, as perforator arteries originating from a lateral DIEA branch may not provide flap perfusion across the midline.

The vascular pedicle of the harvested DIEP flap can be described as having five possible arterial segments (Figure 2):

- (1) DIEA segment deep to the rectus abdominis
- (2) DIEA segment within the rectus muscle (intramuscular)
- (3) intramuscular segment of a perforating artery
- (4) subfascial segment of a perforator
- (5) subcutaneous perforator segment.

Because the perforator size, position and relation to the rectus muscle predict the difficulty of the surgical dissection, demonstrating these features with imaging permits the pre-operative selection and localisation of the optimal perforator. There are five general types of DIEA perforating arteries:

- (1) Perforator with a short intramuscular course (<4cm) through the rectus muscle: these are the easiest and safest to dissect (Figure 3a,b).

Address correspondence to: Dr Lee M Mitsumori, Department of Radiology, University of Washington Medical Center, 1959 NE Pacific Street, Box 357115, Seattle, WA 98195, USA. E-mail: lmits@u.washington.edu

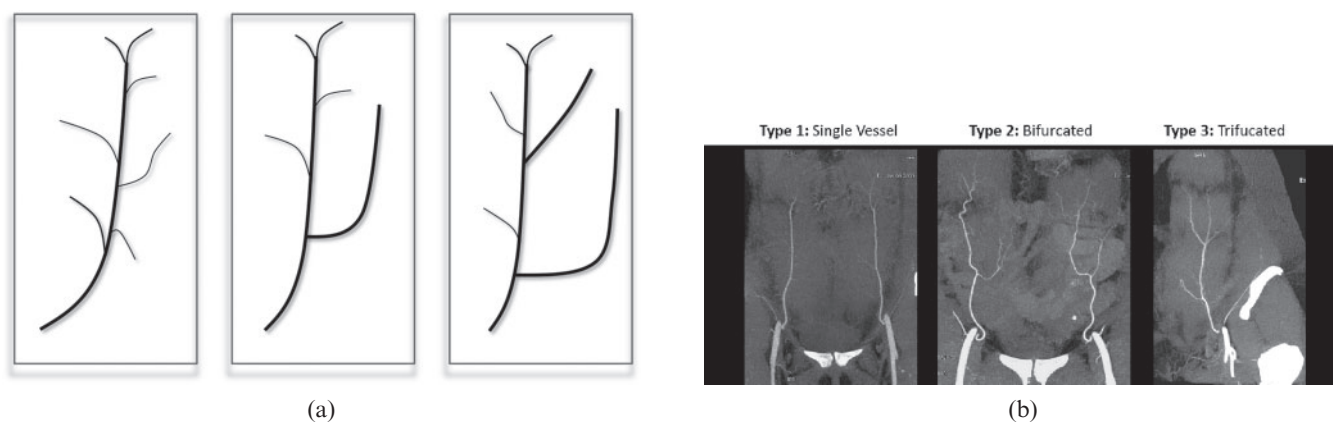


**Figure 1.** Deep inferior epigastric artery (DIEA) branching patterns. Schematic diagrams (a) and coronal CT angiography maximum intensity projection reconstructed images (b) of the three DIEA branching patterns.

- (2) Vessel with a long intramuscular course: these involve more difficult dissection and are prone to injury (Figure 3c,d).
- (3) Perforator with a subfascial segment: a segment of the artery is located just beneath the anterior fascia of the rectus sheath. Careful dissection is required to prevent perforator injury owing to the superficial location (Figure 3e–g).
- (4) Paramedian perforator: this perforates the rectus sheath medial to the rectus muscle. Dissection is straightforward but these can be difficult to find intra-operatively because of the midline location (Figure 3h,i).
- (5) Perforator about a tendinous insertion: the artery courses through or near the tendinous intersection of the rectus muscle and is difficult to dissect owing to the fibrotic environment (Figure 3j–m).

The optimal perforator provides sufficient blood supply to the flap while minimising intramuscular dissection. The desired characteristics of the vascular pedicle for the tissue flap include a large calibre, a central perforator artery location in the flap and a short intramuscular course that is not near a tendinous intersection [6, 7].

### CT imaging

CTA is currently the preferred imaging modality for mapping the DIEA and its perforators. CT has better spatial resolution than MRI, and is more sensitive than ultrasound [2].

Our current protocol is based on a 64-channel platform: craniocaudal helical acquisition from the lesser femoral trochanter to 4 cm above the umbilicus, 0.625×40 mm collimation, pitch 1.375:1, and automatic tube current modulation. Tube potential is selected based on the scan field of view (SFOV) used for the patient: 120 kVp for an SFOV ≥34 cm, and 100 kVp for those <34 cm. Scan timing is achieved with a timing bolus at the level of the acetabulum (region of interest placed in an external iliac artery). The diagnostic scan is initiated at timing bolus peak +10 s after the administration of 100 ml of contrast injected at 5 ml s<sup>-1</sup>.

### Image post processing

The objectives of image post processing are to create rendered and reformatted images that depict the DIEA branching pattern, the size and course of the perforators, and present the location of the perforators for the

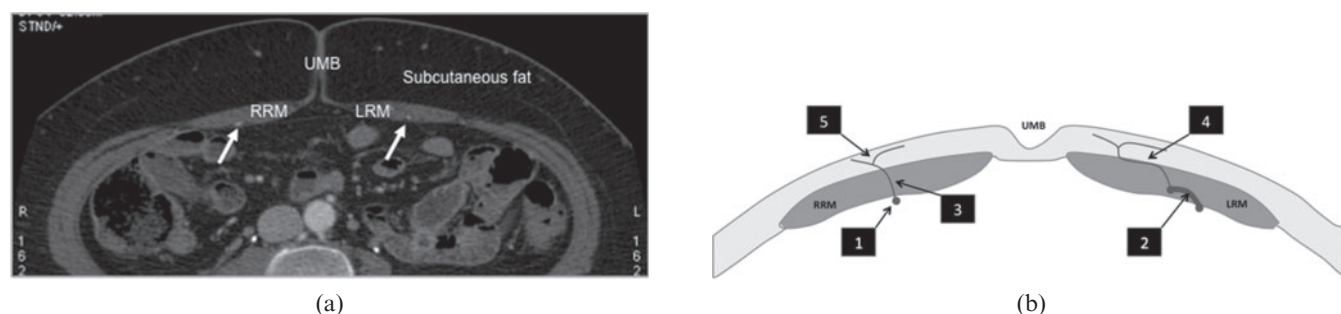


**Figure 2.** A 57-year-old female with breast cancer. Arterial anatomy of the lower abdominal wall. (a) Axial contrast-enhanced CT image through the umbilicus demonstrating the right (RRM) and left (LRM) rectus muscles, the umbilicus (UMB), subcutaneous fat, and the right and left deep inferior epigastric arteries (arrows) located deep in the rectus abdominis. (b) Schematic diagram of the lower abdominal wall depicting the arterial segments of the vascular pedicle used for the deep inferior epigastric artery perforator flap. 1, Deep inferior epigastric artery (DIEA) deep in the rectus muscle; 2, intramuscular segment of a DIEA; 3, intramuscular segment of a perforating branch artery; 4, subfascial segment of a perforator branch artery; 5, subcutaneous perforator segment.

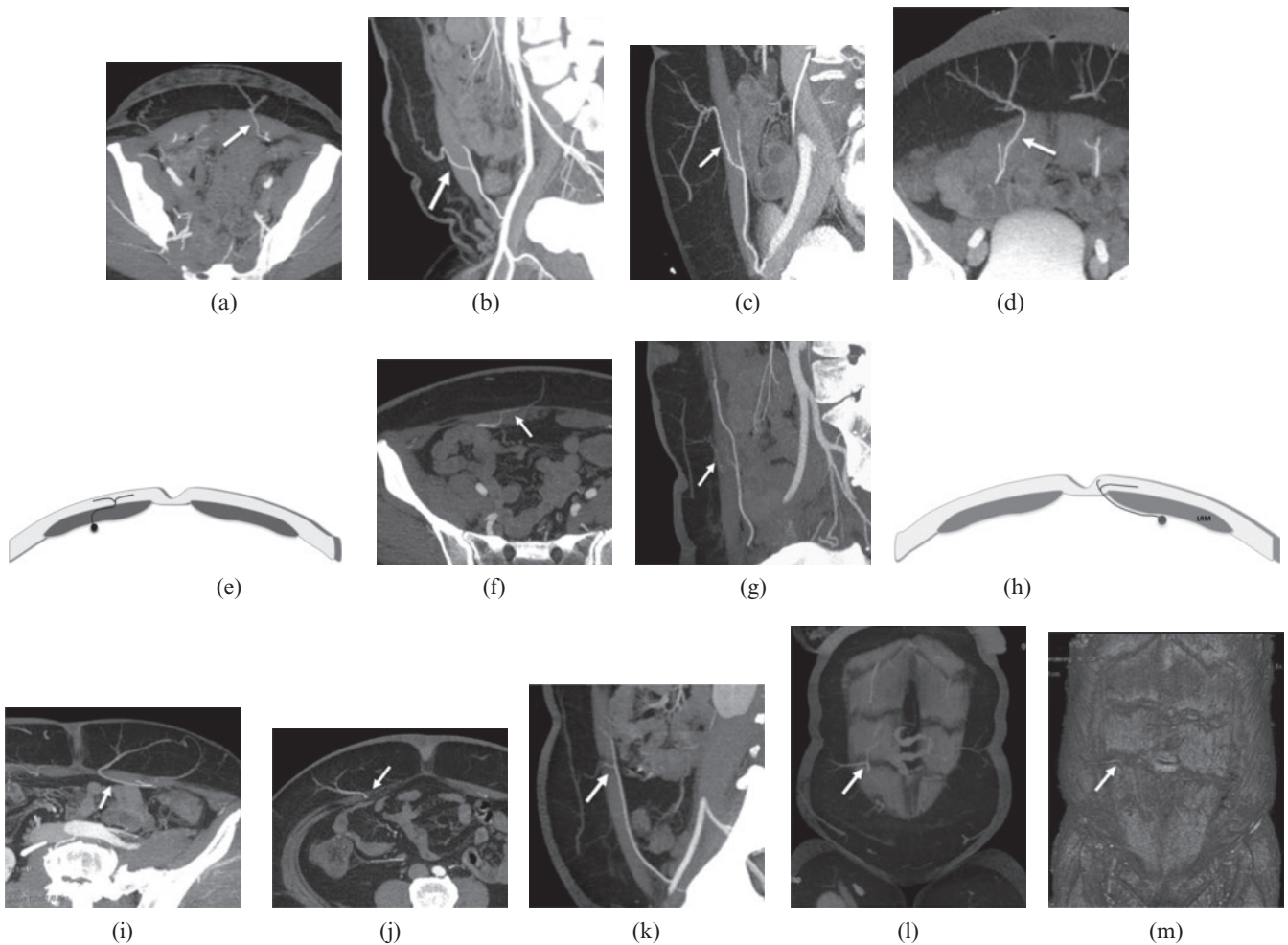


**Figure 3.** Reformatted CT images demonstrating the different types of perforating arteries. (a, b) A 45-year-old female with breast cancer. Axial (a) and sagittal (b) oblique thin maximum intensity projection (MIP) images depicting a perforator with a short intramuscular course (arrows). (c, d) A 53-year-old female with breast cancer. Sagittal (c) and axial (d) oblique thin MIP images showing a perforator with a long intramuscular segment (arrows). (e) Schematic illustrating a right rectus abdominis perforator with a subfascial segment. (f, g) 47-year-old woman with breast cancer. Axial (f) and sagittal (g) oblique thin MIP CT images depicting a perforator with a subfascial segment (arrows). (h) Schematic illustrating a perforator with a paramedian course to the left rectus abdominis muscle (LRM). (i) A 55-year-old female with breast cancer. Axial oblique thin MIP CT image demonstrates a perforator passing medial to the LRM (arrow). (j–m) A 53-year-old female with breast cancer. Axial (j), sagittal (k) and coronal (l) thin MIP reformatted images, and a coronal volume-rendered image (m) to depict a right perforator passing through the tendinous intersection of the right rectus abdominis muscle (arrows).

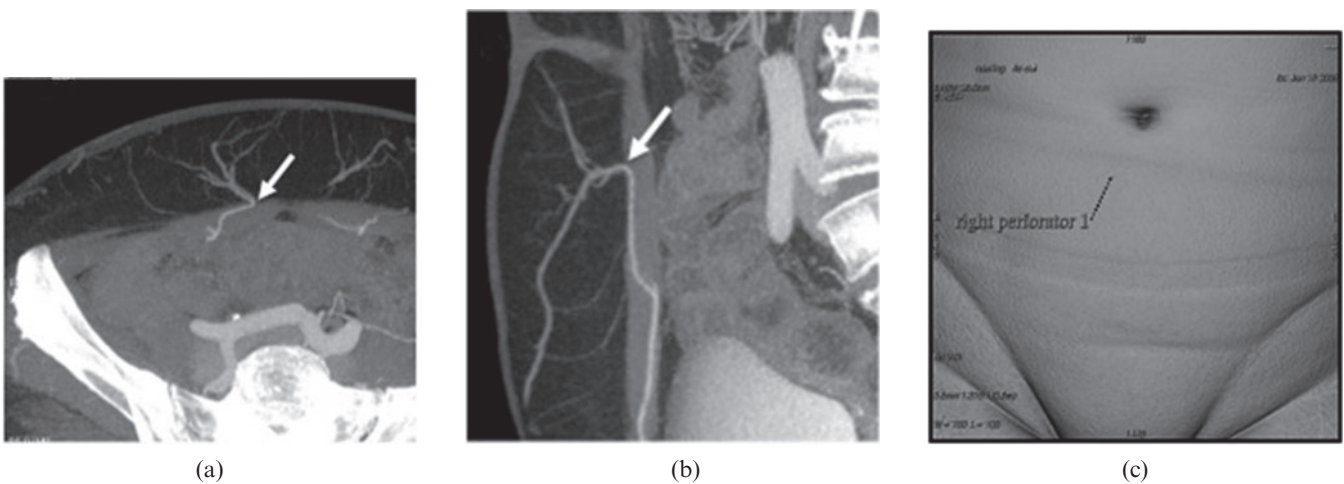


**Figure 4.** A 44-year-old female with breast cancer. Localising the perforator location on the skin view. Site where the perforator exits the anterior rectus fascia (arrows) is identified on the axial (a) and sagittal (b) oblique reformatted images. The three-dimensional cursor is then used to locate and annotate this position on a volume-rendered post-processed image of the skin surface, creating a “skin view” (c).

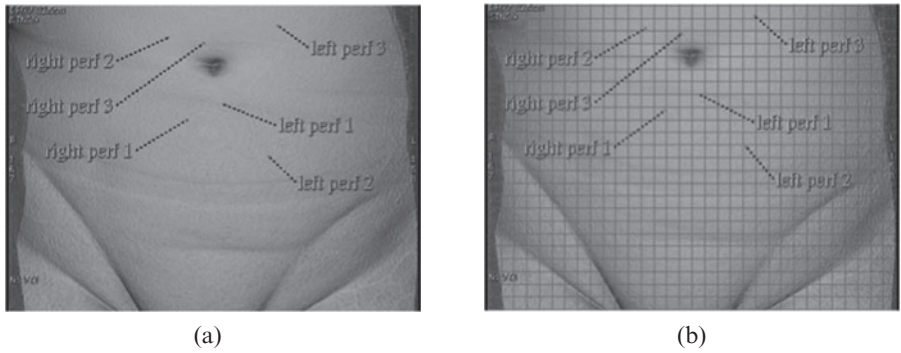


**Figure 5.** A 44-year-old female with breast cancer. Creating the perforator location map. After the sites of the three dominant perforators on the right and left sides of the lower abdomen are marked on the skin view (a), a 1×1 cm grid is superimposed on the skin view (b) to facilitate intra-operative localisation of the selected perforator based on the location relative to the umbilicus.

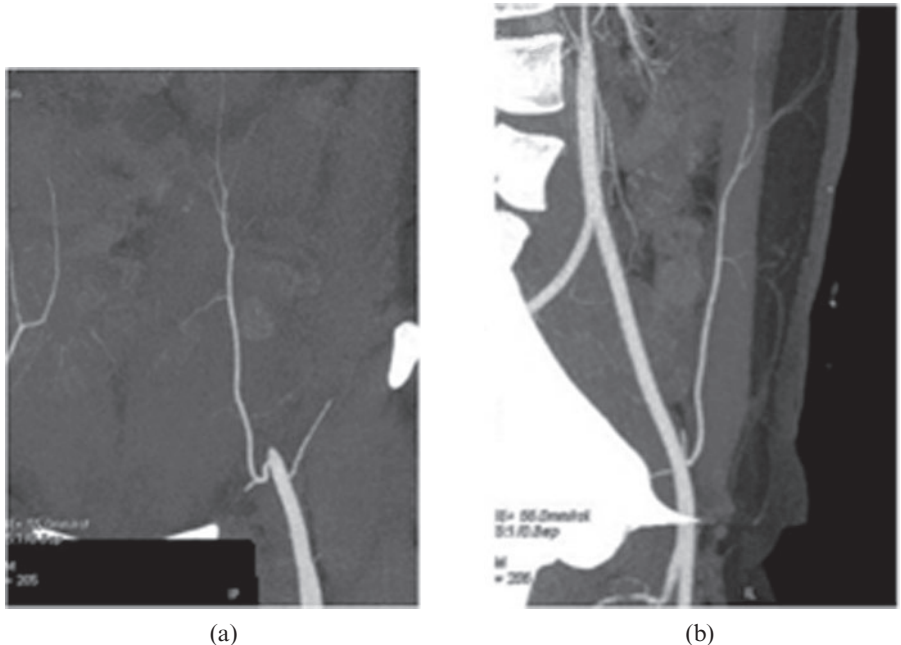


**Figure 6.** A 46-year-old female with breast cancer. Depicting the course and branching pattern of each deep inferior epigastric artery (DIEA). Coronal (a) and sagittal (b) oblique maximum intensity projection (MIP) images are created of a left DIEA to demonstrate the entire course of the vessel in relation to the rectus muscle, and the branching pattern of the artery.

operative dissection [8]. The post-processed images created at our institution include:

- Volume-rendered (VR) image of the skin surface of the lower abdominal wall (skin view) to provide a location map of a perforating artery’s location in relation to the umbilicus (Figure 4c).
- Axial maximum intensity projection (MIP) images to locate the site where a perforator exits the rectus fascia. The perforator exit site is then colocalised with the 3D cursor—which is a standard feature available on commercially available image post-processing platforms—and labelled on the VR skin view (Figure 4a–c).
- Sagittal and axial oblique MIP images of each perforator to demonstrate the calibre and course of the artery (Figure 4a,b). We depict the three largest perforators found within each hemi-abdomen, and label these on the skin view with the largest perforator labelled as Perforator Number 1.
- After the selected perforators are localised on the skin view, a 1×1-cm grid is superimposed on the skin view (Figure 5a,b). This image is used to locate the perforators in the operating room based on their position relative to the umbilicus.

- Sagittal and axial oblique MIP images of the right and left DIEAs to depict their branching pattern and course in relation to the rectus muscle (Figure 6a,b).

**Summary**

CTA with image post processing can be used to depict the branching pattern of the DIEAs and the location, size and course of their perforating arteries. Pre-operative CTA facilitates the selection and intra-operative localisation of the optimal perforator artery by the surgeon, which shortens operative times, improves outcomes and decreases patient morbidity.

**References**

1. Granzow JW, Levine JL, Chiu ES, LoTempio MM, Allen RJ. Breast reconstruction with perforator flaps. *Plast Reconstr Surg* 2007;120:1–12.
2. Rozen WM, Ashton MW. Improving outcomes in autologous breast reconstruction. *Aesthetic Plast Surg* 2009;33:327–35.
3. Clavero JA, Masia J, Larranaga J, Monill JM, Pons G, Siurana S, et al. MDCT in the preoperative planning of abdominal perforator surgery for postmastectomy breast reconstruction. *AJR Am J Roentgenol* 2008;191:670–6.

4. Rozen WM, Ashton MW, Grinsell D, Stella DL, Phillips TJ, Taylor GI. Establishing the case for CT angiography in the preoperative imaging of abdominal wall perforators. *Microsurgery* 2008;28:306–13.
5. Smit JM, Dimopoulou A, Liss AG, Zeebregts CJ, Kildal M, Whitaker IS, et al. Preoperative CT angiography reduces surgery time in perforator flap reconstruction. *J Plast Reconstr Aesthet Surg* 2009;62:1112–17.
6. Phillips TJ, Stella DL, Rozen WM, Ashton M, Taylor GI. Abdominal wall CT angiography: a detailed account of a newly established preoperative imaging technique. *Radiology* 2008;249:32–44.
7. Karunanithy N, Rose V, Lim AKP, Mitchell A. CT angiography of inferior epigastric and gluteal perforating arteries before free flap breast reconstruction. *Radiographics* 2011;31:1307–19.
8. Rozen WM, Garcia-Tutor E, Alonso-Burgos A, Acosta R, Stillaert F, Zubieta JL, et al. Planning and optimising DIEP flaps with virtual surgery: the Navarra experience. *J Plast Reconstr Aesthet Surg* 2010;63:289–97.